VOL. 15, NO. 18, SEPTEMBER 2020 ISSN 1819-6608
ARPN Journal of Engineering and Applied Sciences
©2006-2020 Asian Research Publishing Network (ARPN). All rights reserved.
www.arpnjournals.com

MAGNETIC PROPERTIES AND CRITICAL BEHAVIOR IN $La_{0.66}Ca_{0.33}Mn_{(1-x)}^{4+}Fe_xMn^{3+}O_3$-system: A MONTE CARLO APPROACH

F. F. Jurado-Lasso, N. Jurado-Lasso and J. F. Jurado
Grupo Propiedades Térmicas Dieléctricas de Compositos, Dep. de Ciencias Básicas Universidad Nacional de Colombia, Sede Palmira, Colombia
E-Mail: jfjurado@unal.edu.co

ABSTRACT

Standard Metropolis Monte Carlo (S-MMC) simulations allowed us to calculate magnetization as a function of temperature and magnetic field, for the$La_{0.66}Ca_{0.33}Mn_{(1-x)}^{4+}Fe_xMn^{3+}O_3$($x$=0, 5, 10, 20 and 30 %)(LCMFx) compound. The respective critical exponents for M(T), H/M(H) and M(H,T=T_c) close to the critical temperature, were calculated using the Arrott plot (AP). The values of the critical exponents evinced a type of magnetic universality present in this type of material. The results of the simulation leads us to believe that there is a correlation between the displacement of the magnetic transition temperature (ferromagnetic-paramagnetic), which is characterized by the Curie temperature and an increased percentage of iron present in material. On the other hand, the model determines a value of the critical temperature and this is correlated to the number of Monte Carlo Steps (MCS). For a number of MCS of the order of 10^2, the system tends to relax with the transition temperature which depends on the percentage of iron. By comparing the T_c values determined based on the two methodologies M(T) and AP, we can see that, the greater percentage of iron in the material, the more distance between the two trends. Based on these results, it is possible to infer that the increased percentage of Fe increases the presence of effects in the material that lead to an increased variation of the magnetic anisotropy.

Keywords: monte carlo simulation, manganites, arrott plot, critical exponent.

INTRODUCTION

The interest of the science community is geared towards significantly increasing the use of magnetic refrigeration technology, harnessing the magnetocaloric effect (MCE). The advantages of this technology with respect to conventional refrigeration (compression-evaporation) lies in reducing pollution levels, easy manufacture, and miniaturization, among others. Materials that present MCE are characterized by involving second order phase transitions. For example, in some special cases of ferromagnetic-paramagnetic (FM-PM) type transitions, a correlation has been found between these and the presence of a first ordered phase transition (structural). This correlation can lead to the optimization of the capacity of magnetic refrigeration.

There have been many reports of families of compounds that represent MCE, among which we highlight those known as “Heusler alloys”. For example, MnAs [1], $MnFeP_{1-x}As_x$ [2], Gd5(Si_xGe_{1-x})4 [3], MnNiGe: Fe[4], among others.

Most cases report the substitution of localized ions in lattice sites, which leads to a change in the number of immediate neighbors that present interaction between magnetic ions: for the particular case of *Mn-Mn* type interactions, we assume that these are directly responsible for the magnetic and structural stability of the material. It has been established that these bonds are directly responsible for the more localized magnetism, as a consequence of the configuration of the orbitals *d* of the *Mn* ion [5] ions, whereas for alloys that do not involve *Mn* ions, it is highly probable that there may be mechanisms in which the electrons can be more itinerant [5, 6].

For the perovskites-type family of compounds (manganite) with the formula $Ln_{1-x}A_xMnO_3$ (Ln =rare earth metal and A= divalent element), the physical properties are mainly governed by the strong competition between the double-exchange (DE) ferromagnetic interaction, super-exchange antiferromagnetic interaction, and spin-phonon coupling [7-9]. These interactions are determined mainly by intrinsic parameters such as: ionic radius, disorder, stoichiometry, doping level, among other extrinsic factors such as: pressure and temperature among others [10, 11].

In the semanganites, *Mn* ions play a preponderant role in the DE phenomenon represented by factor Mn^{3+}/Mn^{4+} that correlates the magnetic properties with the itinerant and/or localized electrons. The reports reveal that the research is geared towards the effect of the substitution of the *Mn* ion by transition elements that can coexist with multiple valence, such as: *Cr*, *Co*, *Fe*, among others [12, 13]. Given the closeness of the ionic radii of Mn^{3+} and Fe^{3+}, there has been an intensification of research into manganite–ferrite type compounds $AMn_{1-y}Fe_yO_3$ [14–16]. Most of these seek to find concluding explanations on the incidents of the effect of the substitution of the *Fe*/*Mn* ion on the crystalline order, magnetic properties, and electric charge transport, among others [17, 18]. Advances are being made in the search for new families of compounds of the $Ln_{1-x}A_xMn_{1-y}Fe_yMnO_3$ type, and results have shown that they are very sensitive to the preparation method [19, 20]. In the simulation field for these materials, a recent report shows the effect of iron on the critical temperature in the compound $LaCaMnFeO_3$ [21]. In order to adjust the results, they had to introduce a factor so that the values of T_c coincided with the experimental reports.

This work presents results and discussion of the simulation of the magnetic thermal response close to the transition phase (ferromagnetic-paramagnetic)

©2006-2020 Asian Research Publishing Network (ARPN). All rights reserved.

of$La_{0.66}Ca_{0.33}Mn_{(1-x)}{}^{4+}Fe_xMn^{3+}O_3$ (LCMFx)(x=0,5,10,20 and 30%) compound. The methodology is developed using the Standard Metropolis Monte Carlo (S-MMC) simulations for a 3D classical Hamiltonian-Heisenberg. The critical exponents for M(T), H/M(T) and M(H, T=T_c) are calculated following the Arrott plot (AP) method.

THE MODEL

In ideal conditions the compound $La_{2/3}Ca_{1/3}MnO_3$ crystallizes into a simple cubic structure and a presence of three types of magnetic ions has been identified: $Mn^{4+}{}_{3d}$(s=3/2), $Mn^{3+}{}_{eg}$ and$Mn^{3+}{}_{eg'}$ (s=2). Spin interaction is conceived via double exchange with the respective bonds $M^{3+}{}_{eg'}$-O- $Mn^{3+}{}_{eg}$, $M^{3+}{}_{eg}$ - O - $Mn^{4+}{}_{d3}$ and $M^{3+}{}_{eg'}$ -O- $Mn^{4+}{}_{d3}$ [22, 23]. For the distribution of *Mn* ions throughout the volume, the option proposed by Hotta *el al*. [24, 25] is well accepted. Under the conditions described above, the magnetic response in the model is usually calculated based on the 3D classic Hamiltonian-Heisenberg [26–29].

$$H = -\sum_{<i,j>} j_{ij}\,\vec{S}_i.\vec{S}_j - K_a\sum_i(\vec{S}_i.\vec{a})^2 - \sum_i \vec{S}_i.\vec{h} \qquad (1)$$

For the first term, the sum extends to the closest neighbors with constant interaction J_{ij} between the sites *i* and *j*. It is established that the most relevant interactions are those which occur between three types of ions: $Mn^{4+}{}_{3d}$, $Mn^{3+}{}_{eg}$ and $Mn^{3+}{}_{eg'}$.

Table-1. Exchange parameters J_{ij} used in the model.

Bond	J_{ij}(meV)
Mn^{4+} - $Mn^{3+}{}_{eg}$	7.6
Mn^{4+} - $Mn^{3+}{}_{eg'}$	3.8
$Mn3^{+}$ - $Mn^{3+}{}_{eg'}$	4.65
$Mn^{3+}{}_{eg}$- Fe^{3+}	-4.95
$Mn^{3+}{}_{eg'}$- Fe^{3+}	-1.95

The second term involves crystalline anisotropy along the easy axis (K_a= 1.24844 meV). The third term refers to the Zeeman Interaction. The proposal considers the substitution of the manganese ion for iron in the following compound $La_{0.66}Ca_{0.33}Mn_{(1-x)}{}^{4+}Fe_xMn^{3+}O_3$($x$=0, 5, 10, 20 and 30 %). Despite the complex electronic configuration of iron, the substitution of a high-spin ion is more likelyFe^{3+}($t^3{}_{2g}e_g{}^2$:s=5/2), justified by the fact that there is greater favorability with respect to a low-spin iron.

Table-2. Model parameters for the number Mn^{4+} atoms per unit cell.

x(%)	Fe^{3+}	Mn^{4+}	Mn^{3+}
0	0	33	66
5	90	28	66
10	225	23	66
20	450	13	66
30	1350	3	66

SIMULATION

For a three-dimensional simple cubic lattice, the periodic boundary conditions are determined only for nearest neighbor interactions. The transverse direction has been taken as plane *xy*, whereas the direction perpendicular to the film is axis *z*. The volume of the sample considered was $V = (30)^2 5(u.c)^3$ (unit cells), for a total of N=4500 atoms. In this way, we multiply all the exchange constants listed in the Table-1. Of this total of atoms, only 33% correspond to Mn^{4+}, with the presence of iron, this total varies (see Table-2). A simulation was carried out of the cooling process in the temperature range with the extremes slightly distanced from the critical temperature. A configuration of fixed spins aligned along the *j* axis is assigned, as a starting point. Magnetization per site is calculated based on expression.

$$\vec{m} = \frac{1}{N}\sum_i \vec{s}_i \qquad (2)$$

The average thermal equilibrium is established based on the critical temperature value reported for this material in the absence of iron. For simulation model, it was identified that critical temperature value correlates with the number of Monte Carlo Steps (MCS). For a number of MCS of the order of 10^2, the system tends to relax with a transition temperature that depends on the *%Fe* content. The acceptance or rejection of a change of a spin of an assigned site is governed by the transition probability $W = min(1, exp[-\Delta H/KT])$. The critical temperature value was assessed from the position of the maximum of the specific heat curves (not shown here).

NUMERICAL RESULTS AND DISCUSSION

Figure-1a) shows the dependence of the magnetization on the temperature in the absence of an external magnetic field for different percentages of *Fe*. The increased ion content shifts the critical temperature towards the lower temperature region following the trend shown in Figure-1b). The magnetic order in the LCMFx compound is affected by the presence and increase of iron ions. The presence of these ions modifies the distance between the ions *Mn/Fe−O*. This effect has also been reported for the following compound types $PrLaCaMnFeO_3$ [31, 32]. In reference [18, 33, 34], it can be inferred that the *Fe* ion does not significantly affect the

©2006-2020 Asian Research Publishing Network (ARPN). All rights reserved.

double exchange mechanism, but it is a fact that it is part of the $Mn^{3+} - O_2 - Mn^{4+}$ chains.

CRITICAL BEHAVIOR STUDY

The magnetic response of the LCMFx compound to an external magnetic field, for temperatures close to the phase transition (ferromagnetic-paramagnetic) was studied based on isotherms M(H) vs H/M, following the Arrott plot (AP) method (Figures 2a, 3a, 4a, 5a and 6a). The methodology followed is shown in the inset of each figure. Spontaneous magnetization Ms(T,0) for LCMFx was obtained through M^2 linearity vs.

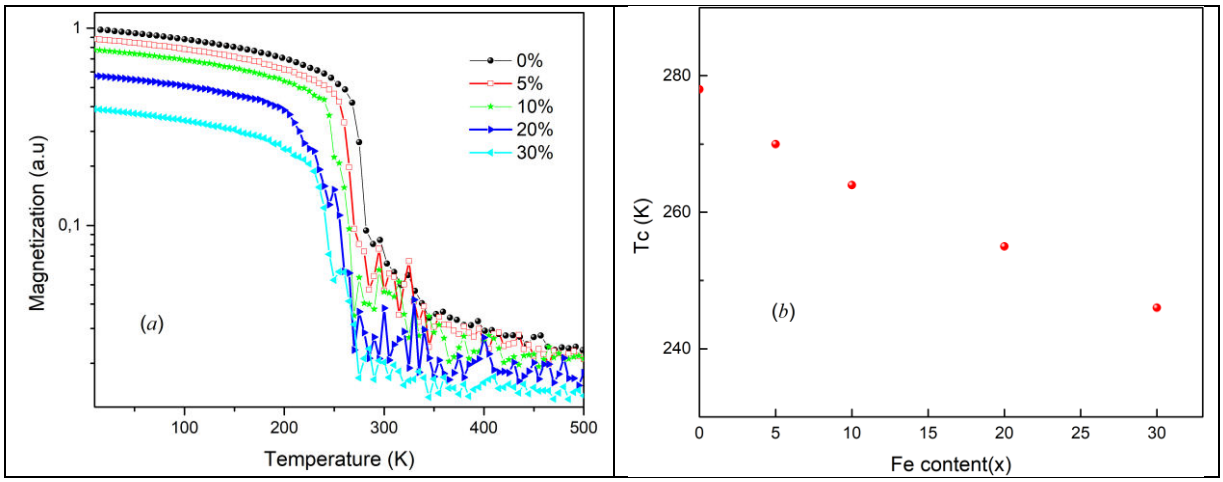

Figure-1. (a) Temperature dependence of the magnetization. (b) Fe content (x) dependent T_c of the $LCMFx(x = 0, 5, 10, 20, 30\ \%)$ compounds.

Table-3. Summary of data calculated at compound LCMFx.

x (%)	T_c(K)	T_c(K)*	β	γ	δ	Ref.
0	278	255	0.414	0.772	7.57	This work
5	270	243	0.431	0.779	6.07	This work
10	264	223	0.420	0.958	5.32	This work
20	255	185	0.493	0.954	4.59	This work
30	246	156	0.414	1.025	4.36	This work
Mean Field Theory			0.5	1	3	[30]
3D Ising model			0.325	1.24	4.82	[30]
3D-Heisenber			0.365	1.336	4.80	[30]

Arrott's Plot

H/M extrapolated towards the ordinate, whilst H/M is determined based on the interception with the abscissa. Figures 2b, 3b, 4b, 5b and 6b show the trend of M_s^2 and H/M with the temperature for LCMFx. By comparing the values of Tc determined based on M(T) and Arrott plot (see Figure-7f), it is possible to see that there is dispersion in the two trends and this becomes more considerable when the percentage of iron increases. This may be associated to an increase of effects that cause great variations in the entropy. This trend can also be seen in other families of compounds [35]. The critical behavior close to the transition phase of compounds LCMFx was characterized through the critical exponents: β,γ, and δ. Associated to spontaneous magnetization Ms(T), reciprocal susceptibility of ($\chi_0(T)$) and isotherm M(H) for T=T_c, In accordance with the staggering hypothesis, these magnetic magnitudes can be written as [36, 37];

$$M_s(T) = M_0(-\varepsilon)^{\beta} \quad \varepsilon < 0$$
$$\chi^{-1}(T) = \frac{h_0}{M_0}(\varepsilon)^{\gamma} \quad \varepsilon > 0 \qquad (3)$$
$$M(T) = D(H)^{\frac{1}{\delta}} \quad T = T_c$$

Where $\varepsilon = \frac{T - T_c}{T_c}$ is the reduced temperature. The constants M_0, h_0/M_0 and D are critical amplitudes. Figures (2c-2d, 3c-3d, 4c-4d, 5c-5d and 6c-6d) show the linear trend of M^2 and H/M with the reduced temperature,

©2006-2020 Asian Research Publishing Network (ARPN). All rights reserved.

respectively. The insets in the figures show the respective adjustment values for critical exponents (see Table-3). The positive slope in the entire range of the calculation implies that the transition here is a second-order transition, according to the Banerjee [38] criteria.

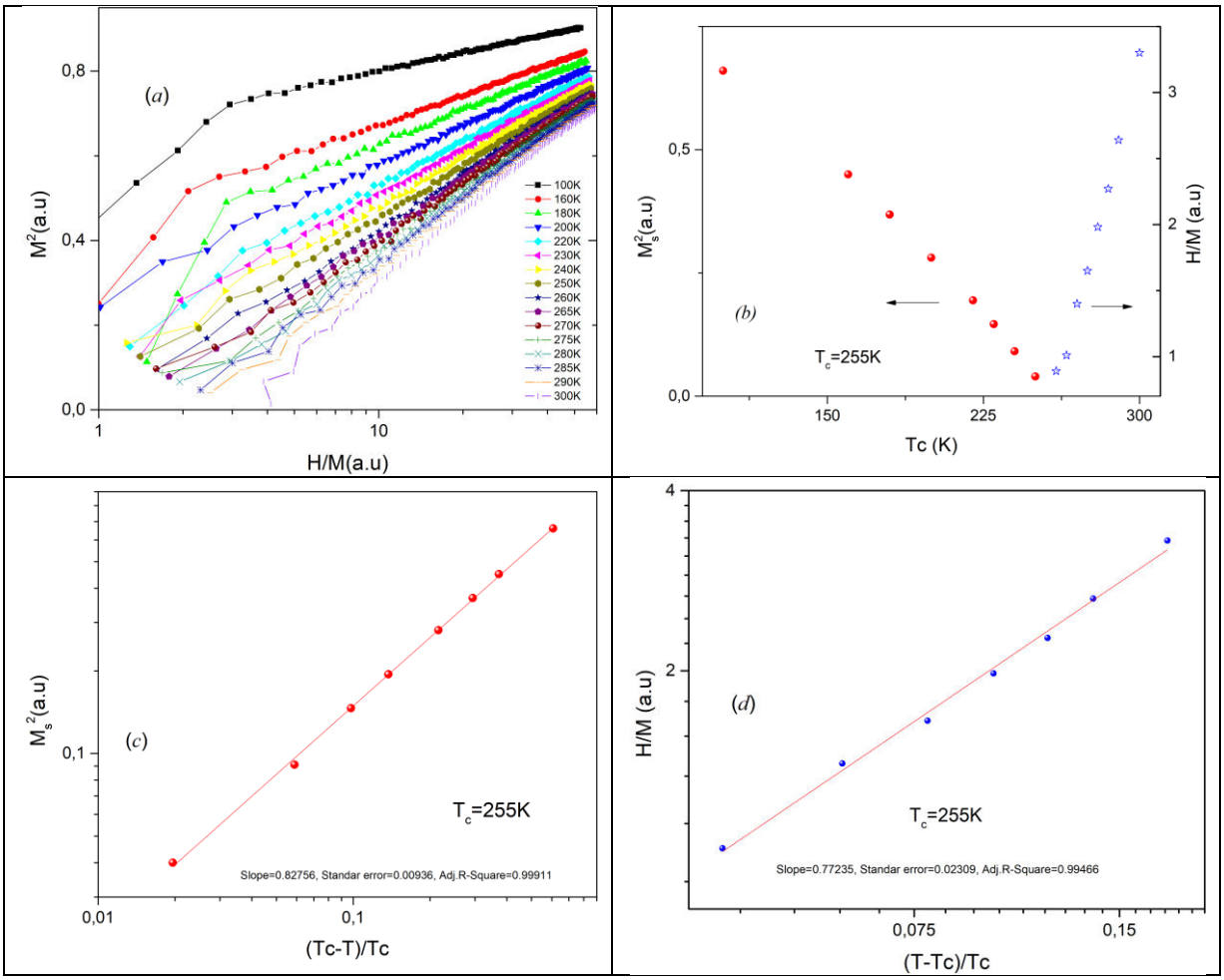

Figure-2. (a) Arrott's plot (M^2 versus H/M) for the *LCMFx*(x = 0%) compound. (b) Temperature dependence of the spontaneous magnetization Ms and reciprocal of susceptibility, respectability. (c,d) Reduced temperature dependence of the spontaneous magnetization Ms and reciprocal of susceptibility H/M. Straight solid lines denote the fitted linear dependence. The inset shows the fitting data.

©2006-2020 Asian Research Publishing Network (ARPN). All rights reserved.

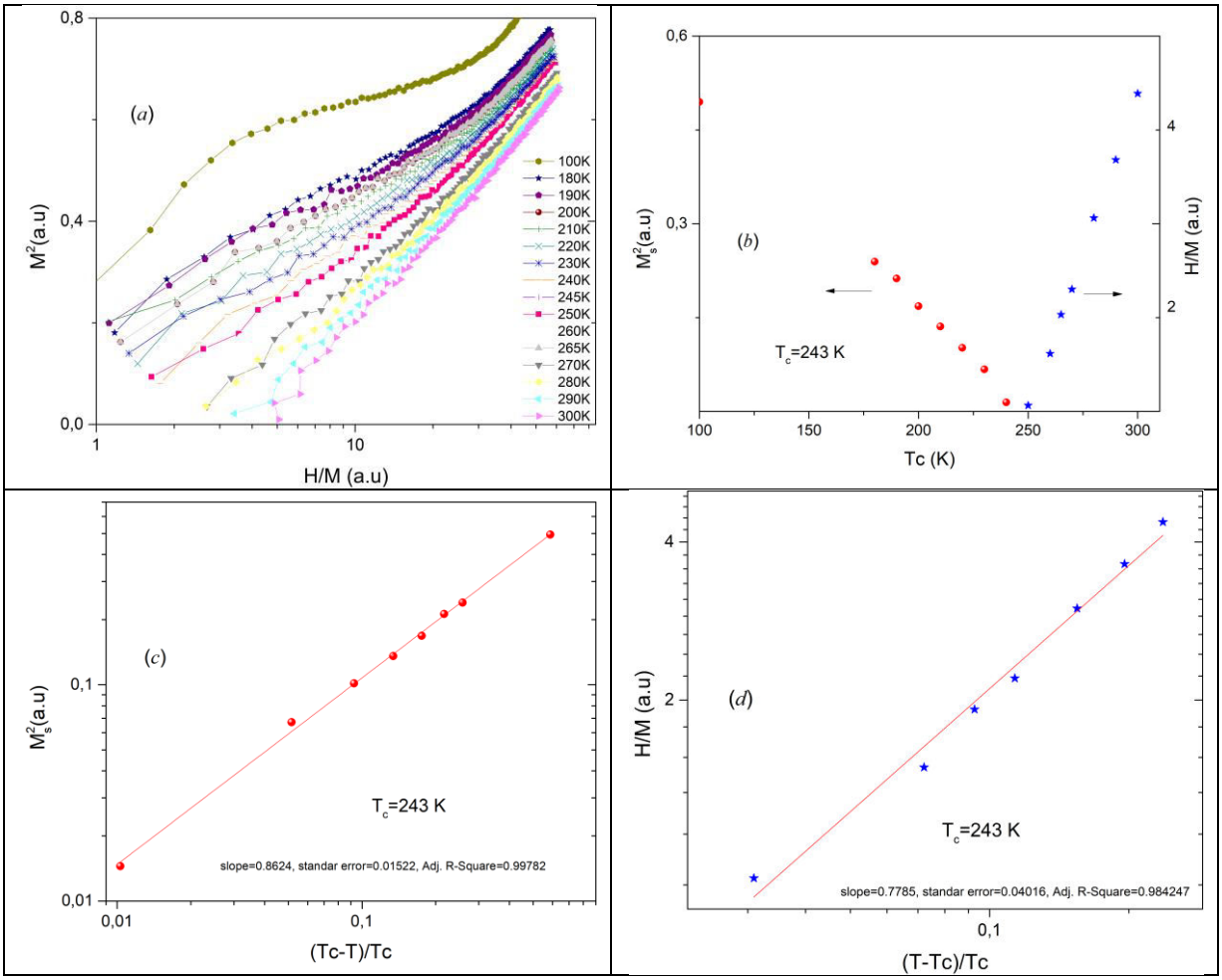

Figure-3. (a) Arrott's plot (M^2 versus H/M) for the *LCMFx*(x = 5%) compound. (b) Temperature dependence of the spontaneous magnetization Ms and reciprocal of susceptibility, respectability. (c, d) Reduced temperature dependence of the spontaneous magnetization Ms and reciprocal of susceptibility H/M. Straight solid lines denote the fitted linear dependence. The inset shows the fitting data.

©2006-2020 Asian Research Publishing Network (ARPN). All rights reserved.

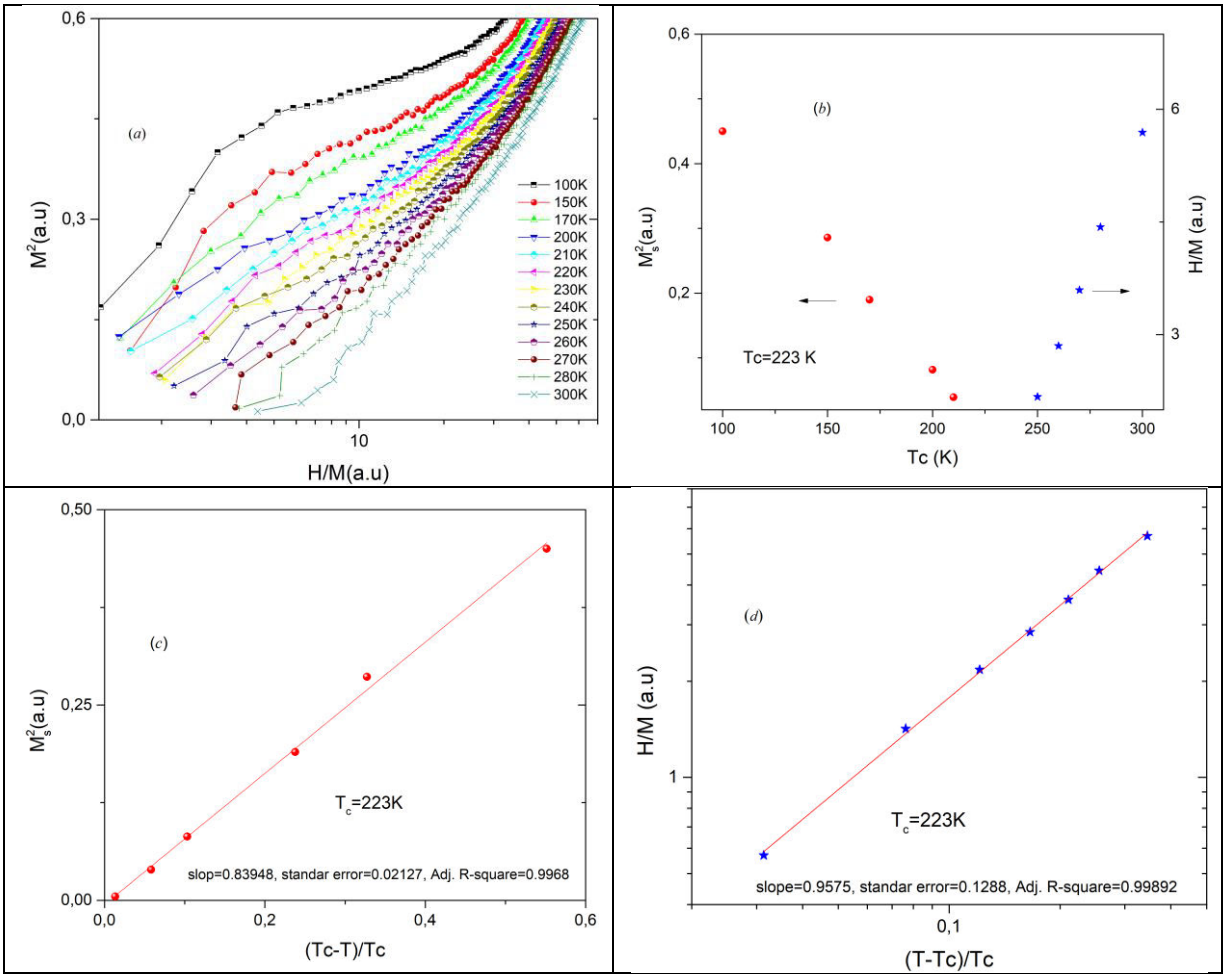

Figure-4. (a) Arrott's plot (M^2 versus H/M) for the *LCMFx*(x = 10%) compound. (b) Temperature dependence of the spontaneous magnetization Ms and reciprocal of susceptibility, respectability. (c, d) Reduced temperature dependence of the spontaneous magnetization Ms and reciprocal of susceptibility H/M. Straight solid lines denote the fitted linear dependence. The inset shows the fitting.

©2006-2020 Asian Research Publishing Network (ARPN). All rights reserved.

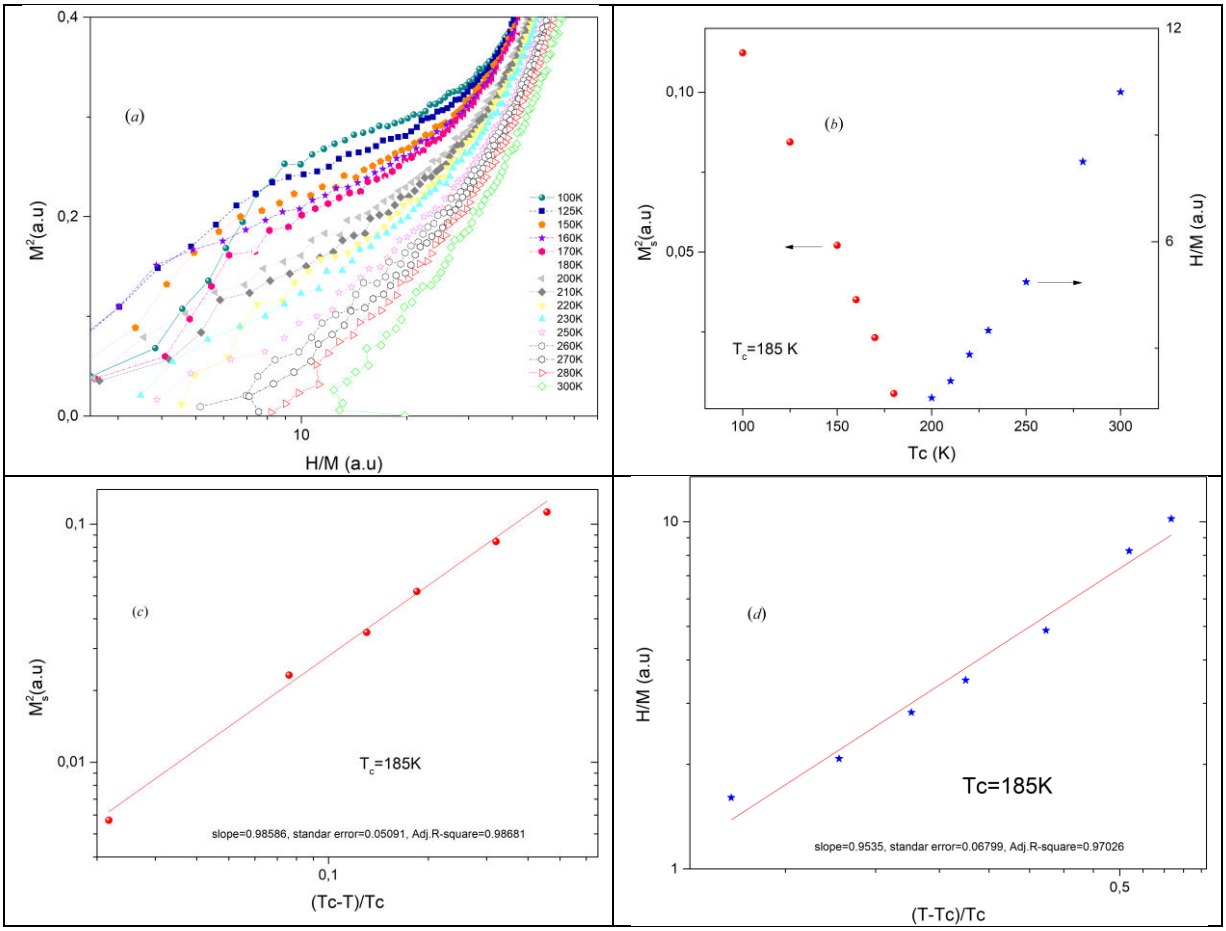

Figure-5. (a) Arrott's plot (M^2 versus H/M) for the *LCMFx*(x = 20%) compound. (b) Temperature dependence of the spontaneous magnetization Ms and reciprocal of susceptibility, respectability. (c, d) Reduced temperature dependence of the spontaneous magnetization Ms and reciprocal of susceptibility H/M. Straight solid lines denote the fitted linear dependence. The inset shows the fitting data.

©2006-2020 Asian Research Publishing Network (ARPN). All rights reserved.

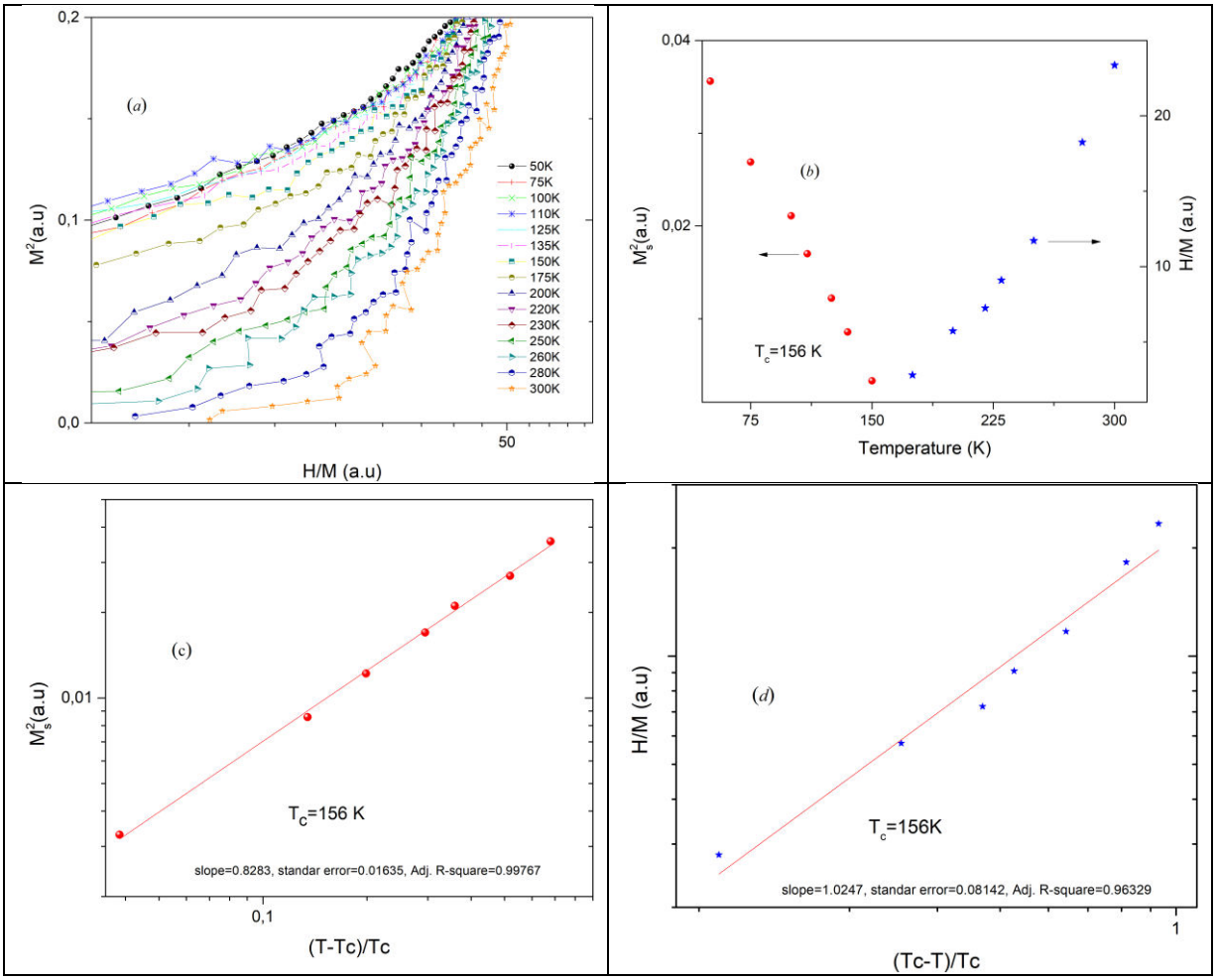

Figure-6. (a) Arrott's plot (M^2 versus H/M) for the *LCMFx*(x = 30%) compound. (b) Temperature dependence of the spontaneous magnetization Ms and reciprocal of susceptibility, respectability. (c, d) Reduced temperature dependence of the spontaneous magnetization Ms and reciprocal of susceptibility H/M. Straight solid lines denote the fitted linear dependence. The inset shows the fitting data.

©2006-2020 Asian Research Publishing Network (ARPN). All rights reserved.

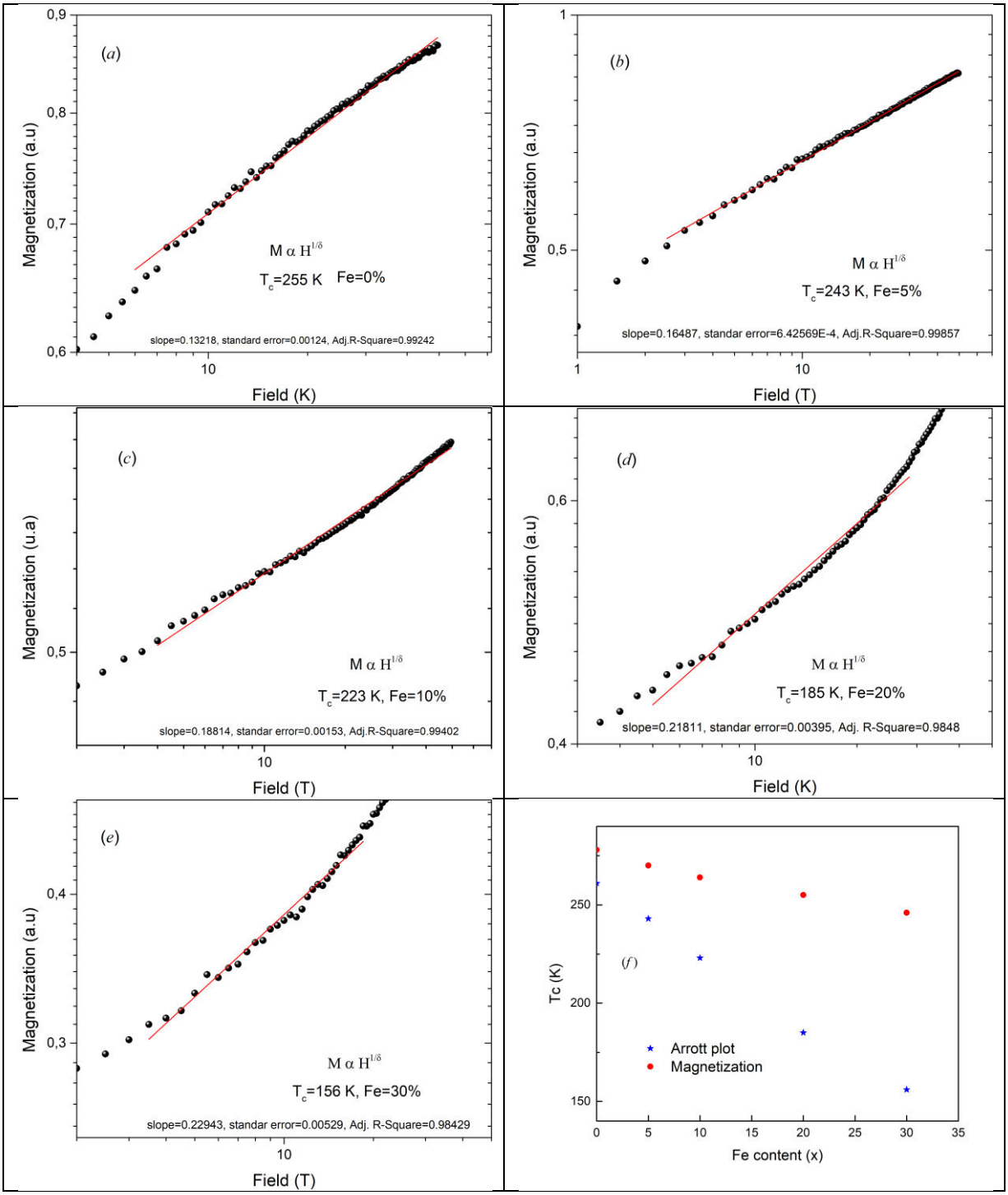

Figure-7. Variation of magnetization M as a function of applied field at $T=T_c$ for LCMFx compounds for: (a)x=0, (b)x=5, (c) x=10, (d)x=20 and (e)x=30%. Straight solid lines denote the fitted linear dependence. The inset shows the fitting data. (f) Fe content (x) dependent T_c to the two formalism; magnetization and y Arrott's plot for LCMFx compounds.

On the other hand, the nonlinear curves (downward curvature even at a high field) indicate that the magnetic response of the compounds distances itself a little from the ideal average field model (β=0.5 and γ=1.0). This trend is usually associated with the presence magnetic anisotropy effects [39-41], as well as the presence of order/disorder effects in the material. However, despite the lack of linearity in the trend, it is possible to infer the presence of a short-range magnetic order in the compounds. Based on the log ($M(H)$) isotherm vs. log$H$a respective critical temperature for each content value for *Fe* (Figure-7), it is possible to determine the critical exponent δ. The corresponding value was calculated with a good level of refinement (see Table-3).

©2006-2020 Asian Research Publishing Network (ARPN). All rights reserved.

The non-linearity in the trend with regards field-dependent magnetization applied for a greater percentage of iron corroborated the increased presence of the effects of magneto crystalline anisotropy that give rise to great entropy variations. By comparing the values of the critical exponents calculated here, with those reported in the references for other materials and models (see Table-3), it is possible to see that the magnetic order of these compounds adjust to the kind of universality surrounding magnetic responses to thermal-magnetic effects.

CONCLUSIONS

The results obtained by Monte Carlo simulation using the Standard Metropolis Monte Carlo (SMMC) simulations for LCMFx compounds, where the only ions replaced are the *Fe* by Mn^{+4}, showed correlation between the displacement of the magnetic transition temperature (ferromagnetic -paramagnetic) that is characterized by the Curie temperature, and the increased levels of *Fe* present in the material. The model is optimized for MCS of the order of 10^2 and the system tends to relax with a transition temperature that depends on the *Fe* content. The critical behavior close to the second-order transition, showed universal behavior, evinced by the critical exponents of: spontaneous magnetization $M_s(T)$, reciprocal magnetic susceptibility $H/M(H)$, and isotherm $M(H,T = T_c)$. The difference of T_c with the *Fe* content for procedures $M(T)$ and Arrott plot, can be indicative of great entropy variations in the compound whose effect can be used in magnetic refrigeration.

REFERENCES

[1] S. Gama, Adelino A. Coelho, Ariana de Campos, A. Magnus G. Carvalho, Flavio C. G. Gandra, Pedro J. von Ranke and Nilson A. de Oliveira. 2004. Pressure-induced colossal magnetocaloric effect in Mn As. Phys.Rev.Lett. 93:237202-237205.

[2] E. Bruck, M. Ilyn, A.M. Tishin and O. Tegus. 2005. Magnetocaloric effects in MnFe1-xPxAs-based compounds. J. Magn. Magn. Mater. 290-291: 8-13.

[3] V.K. Pecharsky, K.A. Gschneidner and Jr. 1997. Giant magneto caloric effect in Gd5(Si2Ge2). Phys. Rev. Lett. 78: 4494-4497.

[4] S. Stadler, M. Khan, J. Mitchell, A.M. Gomes N. Ali, I. Dubenko, A. Y. Takeuchi, and A.P. Guimaraes. 2006. Magnetocaloric properties of Ni2Mn1-xCuxGa. Appl. Phys. Lett. 88: 192511.

[5] E. Bruck, O. Tegus, X.W. Li, F.R. de Boer and K.H.J. Buschow. 2003. Magnetic refrigeration towards room temperature applications. Physic B: Condensed Matter. 327: 431-437.

[6] V.A. Chernenko. 1999. Compositional instability of β-phase in Ni-Mn-Ga alloys. Scr. Material. 40: 523-527.

[7] C. Zener. 1951. Interaction between the d-shells in the transition metals. ii. Ferromagnetic compounds of manganese with perovskite structure. Phys. Rev. 82: 403-405.

[8] A.J. Millis, P. B. Littlewood and B.I. Shraiman. 1995. Double exchange alone does not explain the resistivity of La1-xSrxMnO33. Phys. Rev. Lett. 5144-5147, 74.

[9] J.B. Goodenough, A. Wold, R.J. Arnott and N. Menyuk. 1961. Relationship between crystal symmetry and magnetic properties of ionic compounds containing Mn^{3+}. Phys. Rev. 124: 373-383.

[10] R. M' nassri and M. Koubaa W. Cheikhrouhou-Koubaa, N. Boudjada and A. Cheikhrouhou. 2011. Magnetic and magnetocaloric properties of Pr0.6-xEuxSr0.4MnO3 manganese oxides. Solid State Comm. 151: 1579-1582.

[11] R. M' nassri. 2016. Magnetocaloric effect and its implementation in critical behavior study of La0.67Ca0.33Mn0.9Fe0.1O3. Bull. Mater. Sci. 39(2): 551-557.

[12] P. Barahona, O. Pena, A.B. Antunes, C. Campos, G. Pecchi, Y. Moren, C. Moure and V. Gil. 2008. Magnetic properties of Mn-substitutedGdCoxMn1-xO3 and LaCoxMn1-xO3.J. Magn. Magn. Mater. 320: e61-e64.

[13] S. Mahjoub, Mohamed Baazaoui, R. M'nassri, H. Rahmouni, N. ChnibaBoudjada and M. Oumezzine. 2014. Effect ofiron substitution on the structural, magnetic and magnetocaloric properties of Pr0.6Ca0.1Sr0.3Mn1xFexO3 (0 < x <0.075) manganite. J. Alloys Comp. 608: 191-196.

[14] J.M. Barandiarana, J. Gutierrez, L. Righi, M. Amboage, A. Pena, T. Hernandez, M. Insuasti and T. Rojo. 2001. Magnetic properties and magnetoresistance of Bi and Fe substituted manganite. Phys. B: Cond. Matter. 299(34): 286-292.

[15] N.V. Kasper, T. Honig, N. Hamad, K. Barner, G.H. Roa, J.R. Sun, I.O. Troyanchuk and D.D Khalyavin. 2000. Effect of Fe-substitution on charge ordering in

©2006-2020 Asian Research Publishing Network (ARPN). All rights reserved.

Ca-rich manganites Pr1xCaxMnO3. J. Magn. Magn. Mater. 222: 28-32.

[16] G.H. Roa, J.R. Sun, A. Kattwinkel, L. Haupt, K. Baerner, E. Schmitt and E. Gmelin. 1999. Magnetic, electric and thermal properties of La0.7Ca0.3Mn1-xFexO3 compound. Phys. B: Cond. Matter. 269(3-4): 379-385.

[17] R.D. Shannon. 1976. Revised effective ionic radii and systematic studies of interatomic distances in halides and chalcogenides. Acta Crystallogr. A. 32: 751-764.

[18] K.H. Ahn, X.W. Wu, K.Liu, and C.L. Chien. 1997. Effects of Fe doping in the colossal magnetoresistive La1-xCaxMnO3. J. Appl. Phys. 81: 5505-5507.

[19] H.A. Martinez - Rodriguez, J.F. Jurado and E. Restrepo-Parra. 2018. Electrical conductivity behavior of La0.5Ca0.5Mn0.5Fe0.5O3 synthetized by the Solid State Reaction. Modern Applied Science. 12(12): 174-184.

[20] H.A. Martinez-Rodriguez, J.F. Jurado, J. Restrepo, O. Arnache and E. Restrepo-Parra. 2016. Role of iron in the ferromagnetic-antiferromagnetic boundary of La0.5Ca0.5Mn1-xFexO3+d. Ceramics Intern. 42: 12060-12612.

[21] J.D. Alzate-Cardona, H. Barco-Rios and E. Restrepo-Parra. Influence of Fe dope on the magnetocaloric behavior of La2/3Ca1/3Mn1xFexO3 compounds: A Monte Carlo simulation. J. Phys. D: Appl. Phys. 1: 085003(p. 9).

[22] H. Meskine, H. Kronig and S. Satpathy. 2001. Orbital ordering and exchange interaction in the manganites. Phys. Rev. B. 64: 094433-094512.

[23] L.I. Koroleva, D.M. Zashchirinskii, A.S. Morozov and R. Szymczak. 2012. Magnetocaloric effect in manganites. J. Exp. Theor. Phys. 115: 653-661.

[24] E. Dagotto, T. Hotta and A. Moreo. 2001. Colossal magnetoresistant materials; the key role phase separation. Phys. Rep. 344: 1-153.

[25] T. Hotta, Y. Takada, H. Koizumi and E. Dagotto. 2000. Topical scenario for stripe formation in manganese oxides. Phys. Rev. Lett. 84: 2477-2480.

[26] E. Restrepo-Parra, C.M Bedoya-Hincapie, J. Restrepo J.F. Jurado, J.C. Riano Rojas. 2010. Monte Carlo study of the critical behavior and magnetic properties of La2/3Ca1/3MnO3 thin films. J. Magn. Magn. Mater. 322: 3514-3518.

[27] O. Crisan, M. Angelakeris, N.K. Flevaris, N. Sobal and M. Giersig. 2003. Anisotropies in ferromagnetic nanoparticles: simulation and experimental approach. Sens Actuators A. 106: 130-133.

[28] C. Christides, N. Moutis, Ph. Komninou, Th. Kehagias and G. Nouet. 2002. Dependence of exchange bias energy on spin projections at (La,Ca)MnO3 ferromagnetic/antiferromagnetic interfaces. J. Appl. Phys. 92: 397-405.

[29] E. Restrepo-Parra, C. M. BedoyaHincapie, G. Orozco-Hernandez, J. Restrepo and J.F. Jurado. 2011. Monte carlo simulation of magnetotransport properties in La0.67Ca0.33MnO3 (FM) and La0.33Ca0.67MnO3 (AF) thin films. IEEE Transc. Magn. 47(12): 4686-4694.

[30] M. Baazaoui, S. Hcini, M. Boudard and S. Zemni. 2016. Critical behavior near the ferromagnetic-paramagnetic phase transition temperature of Pr0.67Ba0.33Mn1xFexO3(x=0 and 0.005. J. Magn. Magn.Mater. 401: 323-332.

[31] A. Tozria, E. Dhahri and E.K. Hlil. 2011. Impact of vacancy and Na substitutions on the magnetic behavior in polycrystalline La0.8Pb0.2MnO3. Phys Lett. A. 375: 1528-1533.

[32] Krichene, P.S. Solanki, S. Rayaprol, V. Ganesan, W. Boujelben and D.G. Kuberkar. 2015. B-site bismuth doping effect on structural, magnetic and magnetotransport properties of La0.5Ca0.5Mn1-xBixO3. Ceramics Int. 41: 2637-2647.

[33] M.M. Xavier, Jr, F.A.O Cabral, J.H.D. Ara Uacute, J. C. Chesman and T. Dumelow. 2001. Magnetic and transport properties of polycrystalline La0.7Sr0.3Mn1-xFexO3. Phys. Rev. B. 63: 012408 (p. 4).

[34] N. Kumar, H. Kishan, A. Rao and V.P.S. Awana. 2010. Fe ion doping effect on electrical and magnetic properties of La0.7Ca0.3Mn1xFexO3 (0 < x <1). J. Alloy. Comp. 502: 283-288.

[35] M.K. Chattopadhyay, P. Arora and S.B. Roy. 2009. Magnetic properties of the field-induced ferromagnetic state in MnSi. J. Physics: Condens. Matter. 21: 296003 (p. 5).

©2006-2020 Asian Research Publishing Network (ARPN). All rights reserved.

[36] A.C. Abhyankar, Y.T. Yu, Y.K. Kuo, G.W. Huang and C.S. Lue. 2010. Thermal and transport properties of Ni2MnGa1-xAlx alloys. Intermetallic. 18: 2090-2095.

[37] H.E. Stanley. 1971. Introduction to Phase Transitions and Critical Phenomena.

[38] B.K. Banerjee. 1964. On a generalized approach to first and second order magnetic transitions. Phys. Lett. 12(1): 16-17.

[39] R. Jesser, A. Bieber and R. Kuentzler. 1983. Magnetic properties of the order VPt3 alloy ii. Critical behavior around the curie point. J. Physique. 44: 631-636.

[40] Tozria, E. Dhahria, E.K. Hlilb and M.A. Valentc. 2011. Critical behavior near the paramagnetic to ferromagnetic phase transition temperature in La0.7Pb0.3Na0.25MnO3. Solid State Comm. 151(4): 315-320.

[41] R. Reisser, M. Fahnle and H. Kronmuller. 1988. The magnetic phase transition in amorphous Fe90Zr10. J. Magn. Magn. Mater. 75(1-2): 45-52.